A Mössbauer study of Fe_2SiS_4, having the olivine structure: comparison with fayalite and related minerals

1997 J. Phys.: Condens. Matter 9 3943

(http://iopscience.iop.org/0953-8984/9/19/014)

J. Phys.: Condens. Matter **9** (1997) 3943–3953. Printed in the UK PII: S0953-8984(97)77714-2

A Mössbauer study of Fe_2SiS_4, having the olivine structure: comparison with fayalite and related minerals

Tore Ericsson†, Katalin Holényi and Örjan Amcoff

Institute of Earth Sciences, Mineralogy–Petrology, Norbyvägen 18 B, S-75236 Uppsala, Sweden

Received 10 September 1996, in final form 10 February 1997

Abstract. Fe_2SiS_4 has the olivine structure $Pnma$ with $a = 1.2410$ nm, $b = 0.7200$ nm, and $c = 0.5814$ nm at room temperature. The Mössbauer spectrum at 295 K consists of two doublets having centroid shifts (relative to α-Fe) and quadrupole splittings for the two metal positions Fe1 (point symmetry $\bar{1}$) and Fe2 (point symmetry m) of CS(1) = 0.88 mm s^{-1}, QS(1) = -3.21 mm s^{-1}, and CS(2) = 0.92 mm s^{-1}, QS(2) = -2.75 mm s^{-1}. A point charge calculation for the nearest S octahedra gives the Mössbauer asymmetry parameters $\eta = 0.65$ and $\eta = 0.98$ for Fe1 and Fe2 respectively, and $V_{zz} < 0$ for both positions. At approximately 130 K there is an antiferromagnetic transition, and a second transition to a ferromagnetic or ferrimagnetic structure takes place at approximately 30 K. Both magnetic regions show complicated Mössbauer spectra, which require the full Hamiltonian for their analysis. Comparisons are made with Mössbauer results on the related minerals Fe_2SiO_4 (fayalite), $Fe_3(PO_4)_2$ (iron sarcopside), and Fe_2GeS_4.

1. Introduction

Olivines are abundant in nature, and have consequently been much studied using Mössbauer spectroscopy (MS) and other methods in the past. The assignments of paramagnetic Mössbauer patterns to the two metal sites, M1, having an inversion centre, and M2, possessing a mirror plane, have been controversial, but during the last few decades there has been agreement on correlating the wider doublet (at elevated temperatures) to the M2 position (Warburton 1978, Annersten *et al* 1982, Ericsson and Filippidis 1986). The cation partitioning in (Fe, M)$_2SiO_4$, M = Mg, Mn, Ni, Co, and Zn, has also been determined (Annersten *et al* 1984, 1982, Ericsson and Filippidis 1986, Virgo and Hafner 1972), and correlated with ion sizes and crystal-field stabilization energies. Additional information concerning site preferences has been gained by studying iron-containing sarcopsides, (Fe, M)$_3PO_4$, M = Ni or Mn, which crystallize in an olivine-related structure (Ericsson and Nord 1984, Ericsson *et al* 1986). Also the compounds (Fe, M)$_2SiS_4$, M = Mg, Mn, Ni, Co, and Zn, have the olivine structure, and these compounds are currently being studied at our laboratory. Here the pure-iron end member, Fe_2SiS_4, is analysed by MS, and placed in relation to related minerals, especially fayalite (Fe_2SiO_4).

† Fax: +46 18 182591; e-mail: tore.ericsson@geo.uu.se.

0953-8984/97/193943+11$19.50

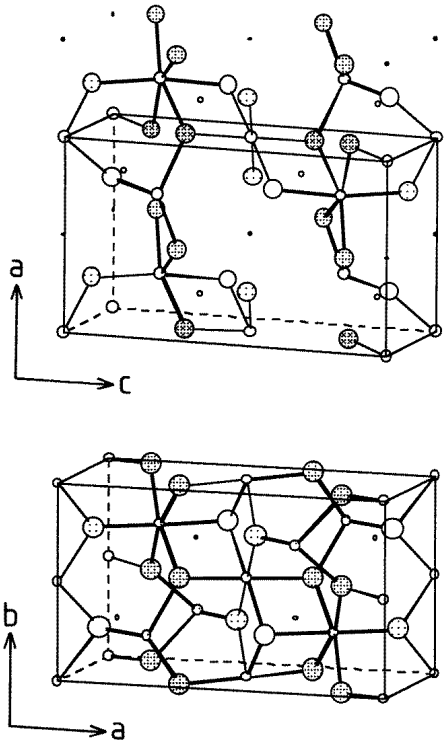

Figure 1. The unit cell of Fe_2SiS_4 (bottom; *Pnma*). Fe1 = white, medium size, point symmetry $\bar{1}$ (e.g. in the middle of the cell and on the faces). Fe2 = lightly dotted, medium size, point symmetry *m*. Si = small open circles. S1, S2, S3 = big circles, white, lightly, and intermediately dotted respectively. The Fe–S nearest bonds are shown by bars. At the top the unit cell for $Fe_3(PO_4)_2$ (sarcopside, $P2_1/c$) is shown for comparison. Here the O1, O2, O3, and O4 atoms are shown as big circles with from light to heavy dotting respectively, and the small black spots represent vacancies. The Fe1 atoms (point symmetry $\bar{1}$) are at the faces, and the Fe2 atoms (point symmetry 1) are grey. In both figures the small open circles represent Si and P respectively. For the sarcopside structure, some atoms and bonds outside the unit cell are shown, to display the Fe2–Fe1–Fe2 trimer arrangement over intervening O1 and O4 atoms. The figure was produced using the program ATOMS from Shape Software.

2. Experimental details

2.1. X-ray diffraction

The instrument was equipped with a graphite monochromator using Cu Kα radiation. Si powder was the calibration standard ($a = 0.543\,0880$ nm), and the goniometer speed was set to 0.6° min^{-1}.

2.2. Sample preparation

The syntheses were performed in evacuated quartz tubes, using 99.999% pure powders of iron, silicon, and sulphur as starting materials. Prior to weighing, the iron was reduced in a hydrogen stream at $\approx$1000 K for two hours to remove oxide traces. The best result was achieved when iron was reacted with sulphur to form FeS_2, which was subsequently

Table 1. Crystal structure data, nearest neighbours, and electric field gradients (point charge calculations) for the minerals discussed. The data for Fe_2SiO_4 are obtained from Smyth (1975), transformed from *Pbnm*, for $Fe_3(PO_4)_2$ from Ericsson and Nord (1984), transformed from $P2_1/a$, for Fe_2GeS_4 from Ericsson and Nord (1995) and Vincent *et al* (1976), and for Fe_2SiS_4 from Vincent *et al* (1976). V_{zz} is given in units of 10^{-20} V m m^{-3}, assuming an anion charge of -2 electrons, using a point charge calculation for the octahedra.

Unit cell	Fe_2SiO_4 *Pnma*		$Fe_3(PO_4)_2$ $P2_1/c$		Fe_2GeS_4 *Pnma*		Fe_2SiS_4 *Pnma*	
a (nm)	1.0471		0.6029		1.2474		1.2407	
b (nm)	0.6086		0.4787		0.7215		0.7198	
c (nm)	0.4818		1.0442		0.5906		0.5812	
β	(90°)		90.97°		(90°)		(90°)	
Bonds in nm	Fe1 $\bar{1}$	Fe2 m	Fe1 $\bar{1}$	Fe2 1	Fe1 $\bar{1}$	Fe2 m	Fe1 $\bar{1}$	Fe2 m
O1, S1	0.2122	0.2221	0.2145	0.2152	0.2477	0.2529	0.2511	0.2548
	0.2122		0.2145		0.2477		0.2511	
O2, S2	0.2131	0.2104	0.2145	0.2116	0.2522	0.2449	0.2508	0.2461
	0.2131		0.2145		0.2522		0.2508	
O3, S3	0.2219	0.2080		0.2025	0.2551	0.2491	0.2533	0.2500
	0.2219	0.2080			0.2551	0.2491	0.2533	0.2500
O3, S3		0.2297		0.2190		0.2629		0.2600
		0.2297				0.2629		0.2600
O4			0.2125	0.2108				
			0.2125					
O4				0.2393				
Average Fe–O, S	0.2157	0.2180	0.2139	0.2164	0.2517	0.2536	0.2517	0.2535
(max − min)%†	4.5%	10.0%	0.9%	17.0%	3.0%	7.1%	1.0%	5.5%
V_{zz}	5.8	3.0	6.9	3.0	−1.8	−0.72	−1.8	−0.64
η	0.95	0.14	0.88	0.47	0.53	0.49	0.65	0.98

†Defined as [(max − min)/average distance] × 100.

mixed with silicon according to: $2FeS_2 + Si = Fe_2SiS_4$ (1–2 g). The mixture was held at 1030 K for four days and at 970 K for ten days before quenching. Typically, all samples contained minute traces of FeS and SiS_2 (at the % level) after the runs, where the latter phase precipitated in the 'cool end' of the quartz capsule, which was ≈3 cm long. However, different heat treatments resulted in nearly identical cell parameters for the Fe_2SiS_4 phase: $a = 1.2410$ nm, $b = 0.7200$ nm, and $c = 0.5814$ nm. These values are in full agreement with the results of Vincent and Bertaut (1976); see table 1.

2.3. Mössbauer spectroscopy

The transmission Mössbauer spectrometer was of constant-acceleration type, using 512 cells for storage of data. The source was Co**Rh** at room temperature, and the calibration was done using natural iron foils as absorbers. The centroid shift (CS) is thus given relative to (the isomer shift of) metallic iron at room temperature. The Mössbauer absorbers were prepared by mixing the material with boron nitride powder, and then pressing the powder to a thin disc. The amount of thiosilicate material used corresponded to less than 5 mg cm^{-2} of natural iron giving 'thin absorbers'; thus there was no need for thickness corrections in the analyses of the spectra. The final Mössbauer analysis was done on 'folded spectra' (256 cells) using a locally developed fitting program with Lorentzian lines, capable of handling

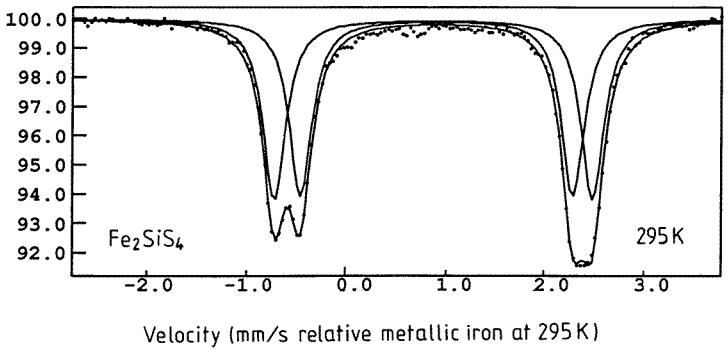

Figure 2. The room temperature Mössbauer spectrum of Fe_2SiS_4, together with the fitted functions.

the full Hamiltonian (Jernberg and Sundqvist 1983). The low-temperature spectra were achieved using a He-flow cryostat (Oxford type) with a precision of ± 1 K.

3. Crystal structure and related parameters

Fe_2SiS_4 is orthorhombic, with space group $Pnma$. The cell edges obtained (at 20 °C), $a = 1.2410$ nm, $b = 0.7200$ nm, and $c = 0.5814$ nm, are to be compared with those of fayalite, having the space group $Pnma$ with $a = 1.0471$ nm, $b = 0.6086$ nm, and $c = 0.4818$ nm (from Smyth (1975); transformed from $Pbnm$). The unit-cell axes are thus ≈20% longer in the sulphur analogue. Relevant data, bond distances, and calculated values of the Mössbauer electric field gradients are given in table 1. The unit cell for Fe_2SiS_4 ($Pnma$) and the related sarcopside structure ($P2_1/c$) are shown in figure 1.

4. Results and discussion

4.1. Mössbauer spectra in the paramagnetic region

At room temperature the Mössbauer spectrum of Fe_2SiS_4 consists of two major profiles, the left-hand one being somewhat split (figure 2). Obviously the spectrum can be decomposed into two doublets in two ways, with 'crossed or overlapped doublets'. However, Mössbauer studies of $(Fe_{0.75}Ni_{0.25})_2SiS_4$ and $(Fe_{0.75}Co_{0.25})_2SiS_4$ at room temperature (to be published elsewhere), showing the same doublets with other intensities due to preferred occupancies, clearly favour the model with overlapping doublets. The two doublets have the same intensity (within the precision of the method, ±1%); thus the two positions have comparable Debye temperatures. The parameters achieved (precision: ± 0.01 mm s^{-1}) for Fe_2SiS_4 at room temperature are, for the two positions (still not correlated to M1 and M2): CS(1) = 0.88 mm s^{-1}, |QS(1)| = 3.21 mm s^{-1}, and CS(2) = 0.92 mm s^{-1}, |QS(2)| = 2.75 mm s^{-1}. The magnitude of QS is the peak splitting in the doublet. The quadrupole splitting is also related to other parameters, through

$$\mathrm{QS} = \frac{eQV_{zz}}{2}\sqrt{1+\frac{\eta^2}{3}}$$

in which the Mössbauer parameters have their conventional meanings.

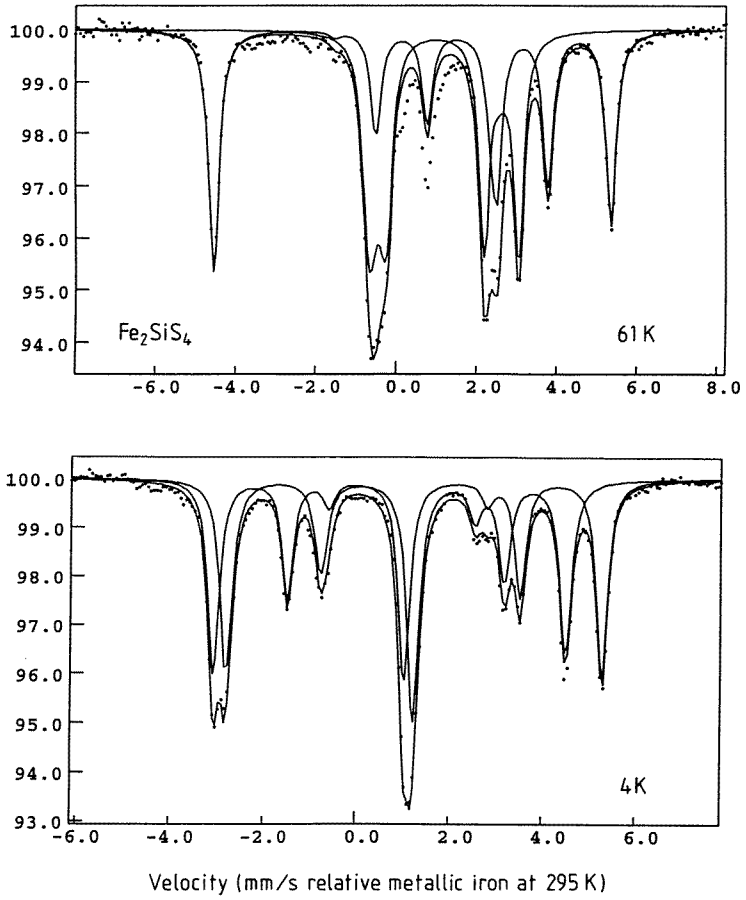

Figure 3. Mössbauer spectra of Fe_2SiS_4 recorded at 61 K (top) and 4 K (bottom) together with fitted functions, obtained using the full Hamiltonian. The misfit in the middle of the upper spectrum is thought to emanate from a paramagnetic impurity phase.

In fayalite, the M2 position gives higher CS and |QS| values at ≈300 °C compared with the M1 position, resulting in a split high-velocity profile (overlapping doublets). At room temperature, the quadrupole splittings are more comparable, but still CS(2) > CS(1), which is also valid at low temperatures (Annersten *et al* 1982). The quadrupole splitting for the M1 position in fayalite thus increases (in magnitude) faster at decreasing temperatures than that for the M2 position. The differences in individual bond lengths for the M1 and M2 octahedra are biggest for the M2 site in fayalite; this is also true for the other compounds discussed here (see table 1). However, other measures such as quadratic elongation or variance of bond angles (Robinson *et al* 1971) indicate the M1 octahedron to be slightly more distorted than the M2 octahedron. From a Mössbauer point of view, a point charge calculation of the electric field gradient created by the octahedral ligands (for an overview, see Travis 1971) should provide a more relevant measure of the distortion (and more specifically, the magnitude of V_{zz}). Such calculations show (see table 1) that the M1 site creates a higher (in magnitude) V_{zz} than the M2 site for all of the minerals studied here. According to Ingalls' theory (Ingalls 1964), an increase in $|V_{zz}|$ from the lattice value will result in a decrease in

|QS| for Fe^{2+}, when the distortion is above a threshold value. Furthermore, a smaller site normally gives a lower value of value of CS. Thus, the assignment of the narrow doublet (having the lower CS) to the M1 site in fayalite is in agreement with these rules of thumb, and the same is also true for the Mössbauer assignments in iron sarcopside, $Fe_3(PO_4)_2$ (Ericsson and Khangi 1988). Using the same argument for the centroid shifts in Fe_2SiS_4 gives that CS(1) should correspond to M1, and CS(2) to M2. The higher magnitude of QS obtained for Fe_2SiS_4 for Fe1 compared to Fe2 could thus be understood as a result of smaller magnitudes of V_{zz} (compared to that of fayalite), giving values below the threshold value in Ingalls' theory.

At around 130 K, there is a magnetic transition, and the variation in CS with temperature is, in the paramagnetic (PM) region, $\approx -1.0 \times 10^{-3}$ mm s^{-1} K^{-1} for both positions, to be compared with the high-temperature limit of the second-order Doppler shift, which is -0.73×10^{-3} mm s^{-1} K^{-1} (Cohen 1976).

4.2. Mössbauer spectra in the magnetic region (30 K–130 K)

There are two magnetic regions of interest, one from ≈30 K to ≈130 K, and the other at lower temperatures. A Mössbauer spectrum recorded at 61 K is shown in figure 3. The complicated spectrum can only be fitted using the full Hamiltonian. Following the procedures of Karyagin (1966) and van Dongen *et al* (1975), CS, QS, and hyperfine-field B-values are obtained as given in figure 4. Note that the QS here in the magnetic region is defined as in the equation above. The magnetic field is much higher for the M1 site than for the M2 site, being ≈27 T for M1 and only ≈4 T for M2 at 30 K. In fayalite at 6 K, the corresponding values are ≈32 and ≈12 T, respectively (Ericsson and Khangi 1988).

4.3. Mössbauer spectra recorded at ⩽30 K

Spectra recorded below 30 K are very different to spectra for the temperature interval above 30 K. A spectrum recorded at 4 K is shown in figure 3. The CS, QS, and B-values are all strongly changed compared to the values obtained for 30–130 K; this might be due to a displacive crystallographic phase transition. However, it is still possible to fit the spectra using two Mössbauer patterns of comparable strength, which hints at other explanations. As it has been established that CS(1) < CS(2), it follows that $B(2) > B(1)$ at the lowest temperatures (≈21 T compared to ≈16 T); see figure 4. The averaged CS value is also lower (≈0.02 mm s^{-1}) below 30 K than that at somewhat higher temperatures, indicating a denser crystal structure, or an increase in the 4s-electron density at the ^{57}Fe nucleus. The large change in B-values indicates a significant change in the electronic structure.

4.4. SQUID data

The magnetization (external field 100 G) versus increasing temperature for a zero-field-cooled sample is shown in figure 5. The signal is nearly constant and weak in the temperature range above 30 K, indicating the magnetic transition at ≈130 K to be of an antiferromagnetic (AFM) type. The transition at around 30 K results in a much stronger signal at low temperatures, indicating the low-temperature material to be ferromagnetic (FM) or ferrimagnetic (FiM). Such a transition could be due to a spin flip; however, the dramatic changes in magnitude of the Mössbauer hyperfine fields at ≈30 K point to more profound changes in the magnetic structure.

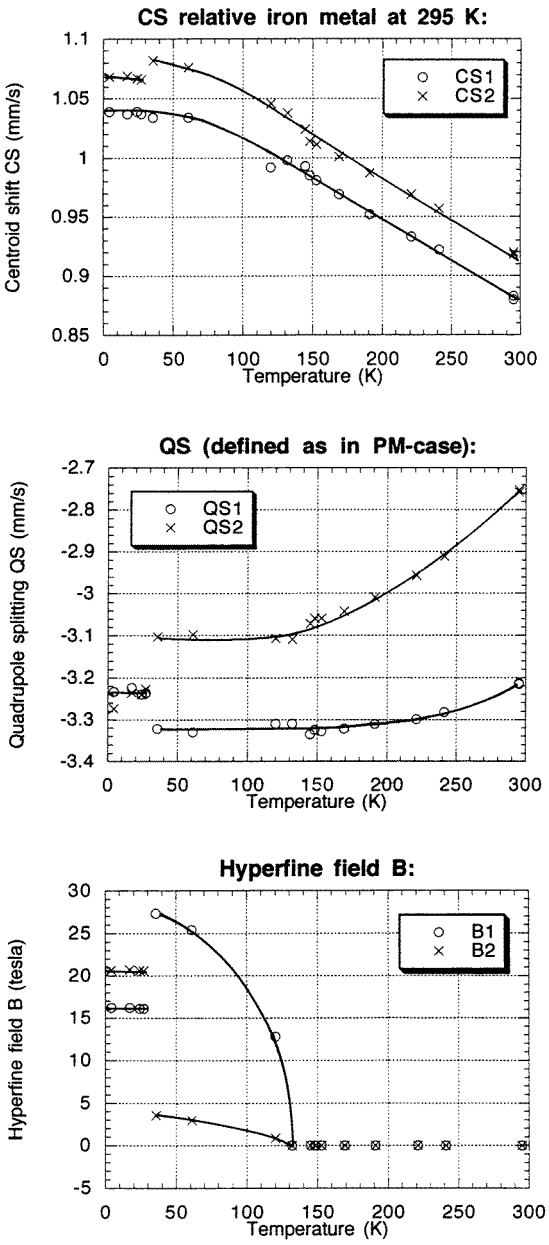

Figure 4. Centroid shifts (CS, top), quadrupole splittings (QS, middle), and hyperfine fields (B in T, bottom) for Fe_2SiS_4, measured at various temperatures. The solid lines are drawn on freehand as guides for the eye.

4.5. Comparison with related structures

At room temperature the CS and |QS| values for the two metal positions are $\approx$1.17 mm s^{-1} and $\approx$2.90 mm s^{-1} for fayalite (Bancroft *et al* 1967) and $\approx$1.2 mm s^{-1} and $\approx$2.95 mm s^{-1} for iron sarcopside (Ericsson and Khangi 1988); thus the CS values are comparable, as expected

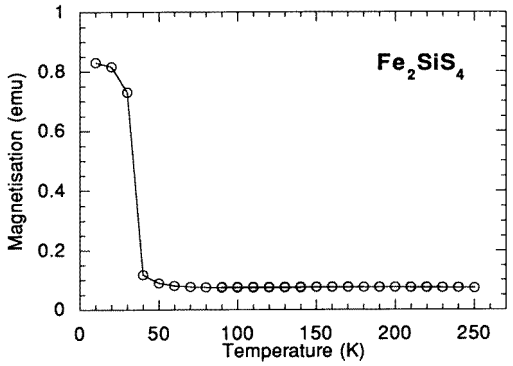

Figure 5. SQUID data (every 10 K) for the magnetization (external field = 100 G) versus increasing temperatures in the interval 10 K–250 K and then at decreasing temperatures down to 90 K for the zero-field-cooled sample.

from the similarity of the sizes of the oxygen octahedra. For the sulphur analogues, the CS values are lower as a result of the more covalent bonding: ≈0.88 mm s^{-1} for Fe_2GeS_4 (two unresolved doublets), which is nearly the same value as obtained above for Fe_2SiS_4. The CS values, as well as showing a difference of ≈0.04 mm s^{-1} between the M1 and M2 positions in Fe_2SiS_4 in relation to averaged bond lengths (see table 1) corresponding to 2.3 mm s^{-1} $Å^{-1}$, are in good agreement with the values and trends found for sulphide minerals in general: ≈2.5 mm s^{-1} $Å^{-1}$) (Vaughan and Craig (1978), p 155). Thus, the mean Fe-anion bond lengths can probably be used as a good measure for predicting CS values for the sulphides studied here. However, for the Ge analogue, the two positions also show comparable |QS| values at room temperature, ≈3.01 mm s^{-1} (Ericsson and Nord 1995), while the doublets are resolved in Fe_2SiS_4 (3.21 mm s^{-1} and 2.75 mm s^{-1}). As the V_{zz}-values are quite comparable for the two compounds (see table 1), it seems that the point charge calculation of V_{zz} gives less quantitative information about the magnitude of QS. The sign of V_{zz}, and the orientation of the electric field gradient principal-axes system (PAS) and the value of the asymmetry parameter η (defined as the ratio $(V_{xx} - V_{yy})/V_{zz}$), are easier to predict than the value of V_{zz} using a point charge calculation. Mössbauer studies on natural single crystals of fayalite indicate $V_{zz} > 0$ for both M1 and M2 (Warburton 1978). Powder MS for synthetic Fe_2SiO_4 as well as $Fe_3(PO_4)_2$ favours $V_{zz} > 0$ for both positions (Ericsson and Khangi 1988), while for Fe_2GeS_4 the fittings indicate $V_{zz} < 0$ (Ericsson and Nord 1995), both findings being in agreement with the above results. A point charge calculation for Fe_2SiO_4, using atoms in the three nearest unit cells, also gave the result in $V_{zz} > 0$ for both positions (Warburton 1978). A fitting of the spectrum recorded at 61 K gives intervals of values of η, Θ, Φ resulting in identical Mössbauer spectra (Karyagin 1966, van Dongen *et al* 1975), with the following results:

Fe1, $V_{zz} < 0$: $(\eta_1 - \eta_2, \Theta_1 - \Theta_2, \Phi_1 - \Phi_2) = (0.6-1, 27^\circ-18^\circ, 12^\circ-84^\circ)$

Fe1, $V_{zz} > 0$: only solutions with $(\eta, \Theta, \Phi) = (\approx 1, 72^\circ, 88^\circ)$

Fe2, $V_{zz} < 0$: $(\eta_1 - \eta_2, \Theta_1 - \Theta_2, \Phi_1 - \Phi_2) = (0.7-0.9, 81^\circ-89^\circ, 13^\circ-67^\circ)$

Fe2, $V_{zz} > 0$: no solutions.

Here Θ and ϕ are the polar and azimuthal angles for the hyperfine field B in the PAS representation. Using the sign of V_{zz} and the value of η as obtained from the point charge

calculation, one gets for Fe1: $V_{zz} < 0, \eta = 0.65$, resulting in $\Theta = 25^\circ$ and $\Phi = 30^\circ$. For Fe2, with $\eta = 0.98$ (see table 1), there is no solution; however, $V_{zz} < 0, \eta = 0.9, \Theta = 89^\circ$ and $\Phi = 67^\circ$ is rather close. In an orthonormal coordinate system oriented as *abc* in *Pnma*, the eigenvectors ($\boldsymbol{e}_{xx}, \boldsymbol{e}_{yy}, \boldsymbol{e}_{zz}$) in the V_{xx}, V_{yy}, and V_{zz} PAS directions have the following coordinates:

Fe1: $\boldsymbol{e}_{xx} = (-0.5789, 0.0205, -0.8151)$

Fe1: $\boldsymbol{e}_{yy} = (0.6321, 0.6428, -0.4328)$

Fe1: $\boldsymbol{e}_{zz} = (0.5151, -0.7658, -0.3851)$

Fe2: $\boldsymbol{e}_{xx} = (0, 1, 0)$

Fe2: $\boldsymbol{e}_{yy} = (0.1938, 0, 0.9810)$

Fe2: $\boldsymbol{e}_{zz} = (0.9810, 0, -0.1938)$.

Thus, the PAS system nearly coincides with the crystal coordinate system for Fe2: $V_{zz} \approx \|$ *a*-axis (deviation 11°); $V_{xx} \parallel$ *b*-axis; $V_{yy} \approx$ *c*-axis (deviation 11°). (One of the axes has to be parallel with the *b*-axis, as there is a mirror-plane perpendicular to the *b*-axis passing through Fe2.) The Θ and Φ values obtained above give the coordinates in the orthonormal crystal coordinate system (Å) for an eigenvector $\boldsymbol{e}_B$ in the hyperfine-field direction:

Fe1(61 K, $V_{zz} < 0, \Theta = 25^\circ, \Phi = 30^\circ$): $\boldsymbol{e}_B = (0.3885, -0.5507, -0.7388)$

Fe2(61 K, $V_{zz} < 0, \Theta = 89^\circ, \Phi = 67^\circ$): $\boldsymbol{e}_B = (0.1955, 0.3907, 0.8995)$.

This clearly indicates that the hyperfine field for Fe2 is not parallel or perpendicular to the *b*-axis; thus the point symmetry for Fe2 is reduced in the magnetic state. Analyses of the spectrum recorded at 4 K give the following intervals:

Fe1, $V_{zz} < 0$: $(\eta_1-\eta_2, \Theta_1-\Theta_2, \Phi_1-\Phi_2) = (0.6-1, 49^\circ-48^\circ, 14^\circ-28^\circ)$

Fe1, $V_{zz} > 0$: $(\eta_1-\eta_2, \Theta_1-\Theta_2, \Phi_1-\Phi_2) = (0.2-1, 66^\circ-70^\circ, 62^\circ-46^\circ)$

Fe2, $V_{zz} < 0$: $(\eta_1-\eta_2, \Theta_1-\Theta_2, \Phi_1-\Phi_2) = (0.6-1, 69^\circ-74^\circ, 6^\circ-22^\circ)$

Fe2, $V_{zz} > 0$: $(\eta_1-\eta_2, \Theta_1-\Theta_2, \Phi_1-\Phi_2) = (0.8-1, 67^\circ-69^\circ, 10^\circ-17^\circ)$.

Fe1, $\eta = 0.65$, $V_{zz} < 0$ now corresponds to

Fe1(4 K, $V_{zz} < 0, \Theta = 49^\circ, \Phi = 17^\circ$): $\boldsymbol{e}_B = (0.0596, -0.3458, -0.9364)$.

Fe2, $\eta = 0.98$, $V_{zz} < 0$ gives

Fe2(4 K, $V_{zz} < 0, \Theta = 74^\circ, \Phi = 22^\circ$): $\boldsymbol{e}_B = (0.3402, 0.8913, 0.2998)$.

However, one has to remember that the atomic positions as well as the crystal structure can be substantially different at low temperatures, making the point charge calculation described above less reliable. A low-temperature neutron diffraction study is under way, and will probably make the situation clearer.

The low-temperature magnetic transition at ≈30 K in Fe_2SiS_4 also has a direct counterpart in Fe_2GeS_4 in the same temperature interval (Ericsson and Nord 1995); however, it is not found in fayalite, even if there are indications of a spin canting at ≈20 K (Kündig *et al* 1967). The magnetic interaction is stronger in the sulphides than in the oxides; the (high-temperature) magnetic transition is at 66 K in fayalite (Kündig *et al* 1967), and at 44 K in iron sarcopside (Ericsson and Khangi 1988), but at ≈150 K in Fe_2GeS_4 (Ericsson and Nord 1995), and at ≈130 K in Fe_2SiS_4. There are also two magnetic regions at low temperature in iron sarcopside. The transition at 44 K is of PM–AFM type (for decreasing temperature); however, iron at the M1 position is still non-magnetic, being magnetic only below 2.4 K

where the two positions show comparable magnetic hyperfine fields (Ericsson and Khangi 1988). The non-magnetic behaviour of Fe1 was described by Warner *et al* (1992) as being a result of frustration. Due to M1 vacancies, there exist Fe2–Fe1–Fe2 trimers (see figure 1) in sarcopside. An AFM coupling of the Fe2 atoms at the ends of the trimers leaves the central Fe1 atom frustrated. This result can be understood by assuming the Fe1–Fe1 interactions (in the absence of vacancies) as well as the Fe2–Fe2 interactions to be stronger than the Fe1–Fe2 interaction. Such a difference in interaction strengths might also be the cause of the two transitions in Fe_2SiS_4.

5. Conclusions

Fe_2SiS_4 has the olivine structure *Pnma* with $a = 1.2410$ nm, $b = 0.7200$ nm, and $c = 0.5814$ nm (precision: ± 0.0001 nm) at room temperature. The Mössbauer spectrum at 295 K consists of two doublets having centroid shifts (relative to α-Fe) and quadrupole splittings (precision: ± 0.01 mm s^{-1}) for the two metal positions Fe1 (point symmetry $\bar{1}$) and Fe2 (point symmetry m) of CS(1) $= 0.88$ mm s^{-1}, QS(1) $= -3.21$ mm s^{-1}, and CS(2) $= 0.92$ mm s^{-1}, QS(2) $= -2.75$ mm s^{-1}, and having asymmetry parameters of $\eta = 0.65$ and $\eta = 0.98$ respectively (from point charge calculations for the nearest S octahedron). At $\approx$130 K there is an antiferromagnetic transition, and a second transition to a ferromagnetic or ferrimagnetic structure takes place at $\approx$30 K (from SQUID data). Both magnetic regions show complicated Mössbauer spectra, which cannot be analysed without using the full Hamiltonian. Comparisons are made with Mössbauer results on the related minerals Fe_2SiO_4 (fayalite), $Fe_3(PO_4)_2$ (iron sarcopside), and Fe_2GeS_4.

Acknowledgments

We are grateful to Dr Per Nordblad, Uppsala, who performed the SQUID measurements, and to Andreas Engel and Peter Scheidler, who, as Erasmus Students from Germany, took part in the measurements. Financial support for this study was obtained from the Swedish Natural Science Research Council (NFR).

References

Annersten H, Adetunji J and Filippidis A 1984 Cation ordering in Fe–Mn silicate olivines *Am. Mineral.* **69** 1110–5

Annersten H, Ericsson T and Filippidis A 1982 Cation ordering in Ni–Fe olivines *Am. Mineral.* **67** 1212–7

Bancroft G M, Maddock A G and Burns R G 1967 Applications of Mössbauer effect to silicate mineralogy—I. Iron silicates of known crystal structure *Geochim. Cosmochim. Acta* **31** 2219–46

Cohen R L 1976 *Application of Mössbauer Spectroscopy* vol 1 (New York: Academic)

Ericsson T and Filippidis A 1986 Cation ordering in the limited solid solution Fe_2SiO_4–Zn_2SiO_4 *Am. Mineral.* **71** 1502–9

Ericsson T and Khangi F 1988 An investigation of $Fe_3(PO_4)_2$-sarcopside between 1.6 K–721 K: comparison with fayalite *Hyperfine Interact.* **40** 783

Ericsson T and Nord A G 1984 Strong cation ordering in olivine-related (Ni, Fe)-sarcopsides: a combined Mössbauer, x-ray and neutron diffraction study *Am. Mineral.* **69** 889–95

——1995 Cation partitioning in olivine-related (Fe, M)$_2GeS_4$ thiogermanates, M = Mg, Mn, Zn *Neues Jahrb. Mineral. Monadsh.* **H5** 202–10

Ericsson T, Nord A G and Åberg G 1986 Cation partitioning in hydrothermally prepared olivine-related (Fe, Mn)-sarcopsides. *Am. Mineral.* **71** 136–41

Ingalls R 1964 Electric-field gradient tensor in ferrous compounds *Phys. Rev.* A **133** 787–95

Jernberg P and Sundqvist T 1983 A versatile Mössbauer analysis program *UUIP-1090* Institute of Physics, University of Uppsala

Karyagin S V 1966 Determination of the local field parameters in Mössbauer hyperfine spectra *Sov. Phys.–Solid State* **8** 391

Kündig W, Cape J A, Lindquist R H and Constabaris G 1967 Some magnetic properties of Fe_2SiO_4 from 4 K to 300 K *J. Appl. Phys.* **38** 947–8

Robinson K, Gibbs G V and Ribbe P H 1971 Quadratic elongation: a quantitative measure of distortion in coordination polyhedra *Science* **172** 567–70

Smyth J R 1975 High temperature crystal chemistry of fayalite *Am. Mineral.* **60** 1092–7

Travis J C 1971 The electric field gradient tensor *An Introduction to Mössbauer Spectroscopy* ed L May (New York: Plenum) p 203

van Dongen T J, Jagannathan R and Trooster J M 1975 Analysis of ^{57}Fe Mössbauer hyperfine spectra *Hyperfine Interact.* **1** 135

Vaughan D J and Craig J R 1978 *Mineral Chemistry of Metal Sulphides* (Cambridge: Cambridge University Press)

Vincent H, Bertaut E F, Baur W H and Shannon R D 1976 Polyhedral deformations in olivine-type compounds and the crystal structure of Fe_2SiS_4 and Fe_2GeS_4 *Acta Crystallogr.* B **32** 1749–55

Virgo D and Hafner S S 1972 Temperature-dependent Mg, Fe distribution in a lunar olivine *Earth Planet. Sci. Lett.* **14** 305–13

Warburton D L 1978 Mössbauer effect studies of olivines *PhD Thesis* University of Chicago, IL

Warner J K, Cheetham A K, Nord A G, von Dreele R B and Yethiraj M 1992 Magnetic structure of iron(II) phosphate, sarcopside $Fe_3(PO_4)_2$ *J. Mater. Chem.* **2** 191–6